Materials Research, Vol. 6, No. 4, 569-576, 2003.

Microstructure and Hysteresis Curves of Samarium-Holmium-Iron Garnet Synthesized by Coprecipitation

Valeska da Rocha Caffarena, Tsuneharu Ogasawara*

COPPE/UFRJ PEMM, Ilha do Fundão
C.P. 68505, 21945-970 Rio de Janeiro - RJ, Brazil

Received: January 23, 2003; Revised: August 4, 2003

An investigation was made into the synthesis and magnetic properties of $Sm_{(3-x)}Ho_xFe_5O_{12}$ (samarium-holmium-iron) garnet ferrite, as yet absent from the literature. The material in question was synthesized by co-precipitation, starting from hydrated chlorides of rare-earth elements and ferrous sulfate, and the mixed hydroxide co-precipitate was calcined at 1000 °C. Using PVA as a binder, rectangular cross section-shaped compacts were produced by means of steel-die pressing, drying and sintering from 1200 to 1450 °C. The main conclusions of this study were that the coercive force decreases as the sintering temperature increases, and that the effect of substituting holmium for samarium in SmIG is entirely different from that provided by replacing yttrium by gadolinium in YIG, which is the most important result of this work. An in-depth investigation will be necessary to determine the correlation between microstructure/magnetic properties and ceramic processing variables.

Keywords: *ceramics, chemical synthesis, electron microscopy, magnetic properties, garnet ferrite*

1. Introduction

Rare-earth garnet-structured ferrites, $R_3Fe_5O_{12}$ (where R is yttrium or a rare-earth cation), continue attracting a great deal of attention[1,2] for both microwave devices and magnetic recording media. Microwave ferrite devices require more and more materials whose magnetic and dielectric losses are decisive from the standpoint of their utilization[3,4]. In this work, the cubic ferrite powder of samarium-holmium-iron garnet $Sm_{(3-x)}Ho_xFe_5O_{12}$ was synthesized and characterized. The literature available on the subject revealed no evidence that this garnet had been previously synthesized. However, based on the existing knowledge about the effect of replacing yttrium by gadolinium in YIG (yttrium-iron-garnet ferrite)[4-6], the replacement of samarium ions by trivalent rare-earth ions such as holmium ions is expected to result in a wide range of properties.

Samarium iron garnet and yttrium iron garnet display almost identical values of spontaneous magnetization in Bohr magnetons per gram molecule *vs.* absolute temperature from zero to about 550 K[4]. In this same temperature range, holmium iron garnet and gadolinium iron garnet are quite similar in their spontaneous magnetization *vs.* temperature curves[5]. The magnetization moment per mole *vs.* absolute temperature curve of the mixed iron garnet $Y_zGd_{(3-z)}Fe_5O_{12}$ (with $0 \leq z \leq 3$) is highly dependent on the z value, the compensation temperatures being 295, 220, 150, and 100 K for z values of 0, 0.6, 1.2, and 1.8, respectively[6]. Hence, similar effects on magnetization-temperature curves would likewise be expected as a result of replacing samarium with holmium in the lattice of samarium iron garnet. The authors of this paper studied $Sm_{(3-x)}Ho_xFe_5O_{12}$ compositions (for x = 0, 1.5, 2.4 and 3.0) and present the results therefrom, illustrated by the case of x = 2.4. The target of this research was a new scientific breakthrough.

2. Experimental Procedure

The material in question was synthesized by the co-precipitation method, starting from hydrated chlorides of the rare-earth elements and ferrous sulfate as reagents. These solutions were all mixed together in a container, the resulting solution presenting a pH value in the range of 2 to 3. This solution was then heated to 105 °C under intensive

*e-mail: valeska@metalmat.ufrj.br

agitation for about 30 min, followed by the addition of KOH to adjust the pH value to 10-10.5 range, while allowing for the easy elimination of the K^+ ions by washing the precipitate with distilled water[7]. A thermodynamic analysis[8] indicated that, for co-precipitation to occur, the final pH should range from 9 to 12; therefore, the synthesization experiment was repeated three times with pH values ranging from 10 to 10.5.

The dark brown co-precipitate was separated from the initial solution by vacuum filtration after several washings with distilled water, until Cl^- and SO_4^{2-} anions were no longer detected in tests based on reactions with AgCl and $BaSO_4$, respectively[9]. The precipitate was dried following Reed's recommendation[10], i.e., initial drying inside a desiccator for 24 h, followed by heating to 75 °C for 4 h. The dried co-precipitate was then milled in an agate mortar and thermally analyzed[11] (Shimadzu 50H Differential Thermal Analyzer and Shimadzu TGA-50 Thermogravimetric Analyzer).

Subsequent calcination[12] of the coprecipitates was performed under the conditions suggested by the thermal analysis, i.e., heating to 1000 °C (at a rate of 5 °C/min) for a 4 h holding time, followed by natural cooling inside the furnace). Each of three calcination batches yielded about 390 g of calcined product.

The brown calcined powder was characterized[13] by X-ray fluorescence (Philips model PW2400 from the Geology and Geosciences Department of the UFRJ; the sample powder was embedded by mixing, pressing and melt-casting into $Li_2B_4O_7$), scanning electron microscopy (Zeiss SEM model DSM 940A, operated at 20 kV to 25 kW, 200 to 20000 times magnification, and Oxford-Link EXL II EDS Module), and X-ray diffraction (Philips PW3170 X-ray Diffractometer, copper K_α [λ = 1.542 Å] radiation, generator operating at 40 kV and 40 mA, scanning 2θ angles from 10 to 100°).

Rectangular cross section ring-shaped compacts (2.0 cm outer diameter, 0.8 cm inner diameter and 0.4 cm height) were produced by dry pressing of the finely milled calcined powder, to which was added an aqueous solution containing 15 wt% of PVA, as a binder, in a suitable amount of PVA (polyvinyl alcohol) corresponding to 2 wt% of the total compacted mass. A total of 50 compacts were produced for each batch.

Ten compacted pieces were sintered, each at 5 different firing temperatures (1200, 1250, 1300, 1400 and 1450 °C), in order to promote the formation of the desired samarium-holmium-iron garnet, according to reaction 1:

$$0.6\ Sm_2O_3 + 2.4\ Ho_2O_3 + 10\ Fe_2O_3 \rightarrow 2\ Sm_{0.6}Ho_{2.4}Fe_{10}O_{24} \quad (1)$$

The firing procedure was performed according to the following heating schedule: 4 °C/min up to 400 °C, a 400 °C plateau for 1 h, 8 °C/min up to the final sintering temperature, at which the sample was kept for 5 h, in air. Cooling was carried out in the furnace at a rate of 8 °C/min down to 800 °C, at which temperature the sample was kept for 1 h before final cooling (at the same rate) to room temperature. Figure 1 shows the thermal profile of the fired ceramic sintered at 1400 °C.

The magnetic properties of the sintered samples were determined using a magnetic hysteresisgrapher (Walker Scientific model AMH-20): each ceramic ring was equipped with varnished copper AWG 29 wire winding to provide a solenoid (magnetically analyzed under a 60 Hz frequency and a 30 Oe maximum magnetic field [except some cases, for which a 100 Oe magnetic field was used]). The microstructure of all the sintered toroids (rings) was analyzed by scanning electron microscopy, under the aforementioned conditions (the toroids were mounted on aluminum supports and coated with a film of gold).

3. Results and Discussion

Figure 2 shows the results of the thermogravimetric and differential thermal analysis. The curve of the thermogravimetric analysis (TGA) indicates a progressive water vapor weight loss from the starting mixture of samarium, holmium and iron hydroxides from room temperature to 500 °C, which amounted to a total of 13.8%. Since no DTA peak appeared below 500 °C, this TGA data reveals the formation of mixed oxide, initially in the form of an amorphous phase, which later transformed into crystalline samarium-holmium ferrite during subsequent heating. The DTA revealed an exothermic peak at 759 °C caused by the transformation of the amorphous mixed samarium, holmium and iron oxides (the amorphous phase) into the crystalline samarium, holmium and iron (III) oxides. The X-ray dif-

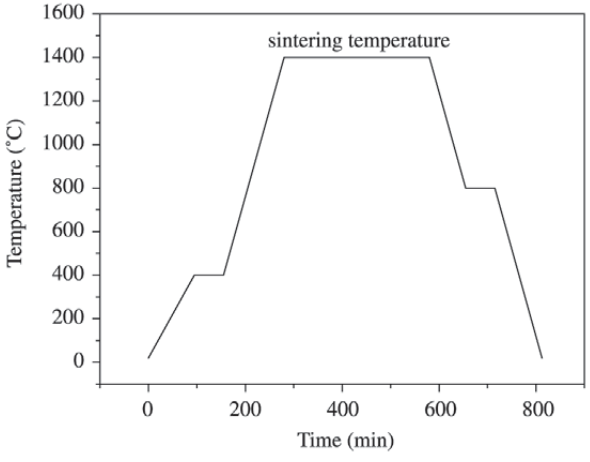

Figure 1. Thermal profile of the fired ceramic sintered at 1400 °C.

fraction pattern of the product calcined at 1000 °C confirmed this transformation, as illustrated in Fig. 3, giving rise to intermediate compounds ($SmFeO_3$, $HoFeO_3$, Fe_2O_3, Sm_2O_3 and Ho_2O_3), which implies the need for longer times and higher temperatures to achieve full conversion of the material to true iron garnet[14,15].

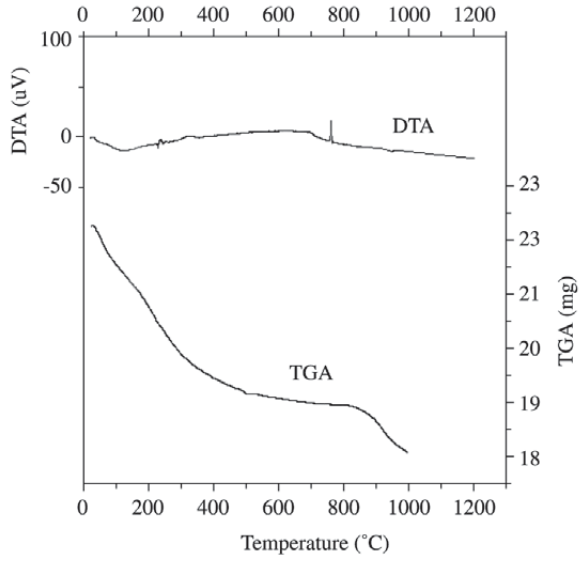

Figure 2. TGA and DTA of co-precipitated samarium, holmium and iron hydroxides with composition $Sm_{0.6}Ho_{2.4}Fe_5O_{12}$, in air, with heating rate of 10 °C/min.

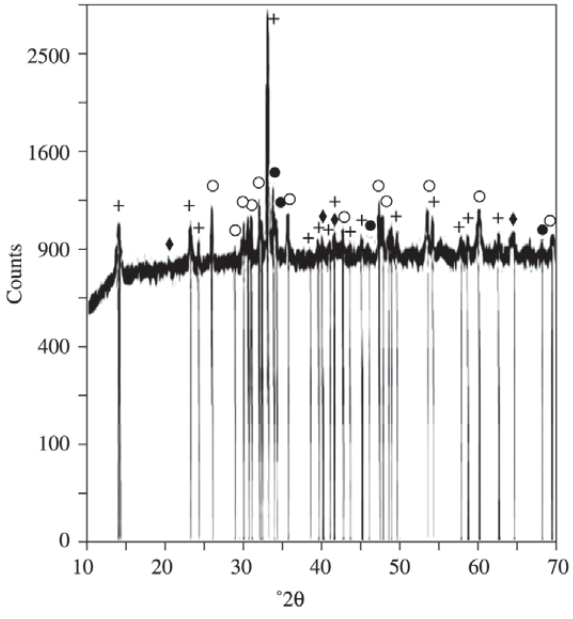

Figure 3. X-ray diffraction pattern of the samarium, holmium, iron co precipitate after calcination at 1000 °C, where + Fe_2O_3, ● $HoFeO_3$, ◯ Sm_2O_3 and ◆ Ho_2O_3.

Figure 4 shows the X-ray diffraction pattern of the mixed oxide sintered at various temperatures in the 1200 to 1450 °C range. As can be seen, the formation of samarium-holmium-iron garnet occurred only at high temperatures. Samarium orthoferrite and simple iron garnets of Sm and Ho ($Sm_3Fe_5O_{12}$ and $Ho_3Fe_5O_{12}$) still remained at 1200 and 1250 °C. At 1300 °C, the values of interplanar distance (d) were in good agreement with *JCPDS* 23-526 data for $Sm_3Fe_5O_{12}$ (lattice parameter, a = 12.530) and *JCPDS* 23-282 data for $Ho_3Fe_5O_{12}$ (lattice parameter, a = 12.376) and orthoferrites were absent. At 1400 °C, some of the peaks were displaced in relation to those of simple garnets. Due to the addition of holmium, these peaks displayed a slight shift (all the peaks shifted similarly under the effect of replacing Sm with Ho) and the reaction of the formation of samarium-holmium-iron garnet was completed at 1450 °C.

In this work, 50 ceramic compacts were produced (10 at

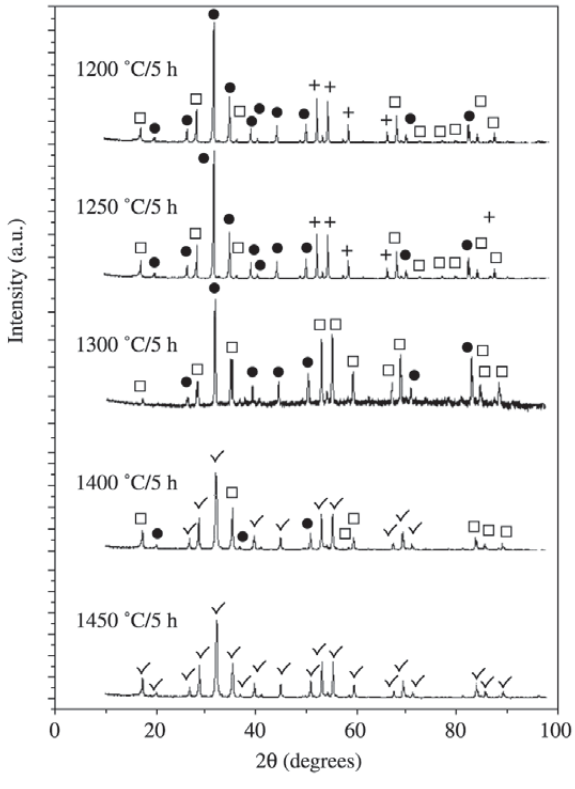

Figure 4. X-ray diffraction pattern of the ceramic pieces sintered at different temperatures in the 1200 to 1450 °C range, where ● $Sm_3Fe_5O_{12}$, □ $Ho_3Fe_5O_{12}$, ✓ $Sm_{0.6}Ho_{2.4}Fe_5O_{12}$ and + $SmFeO_3$.

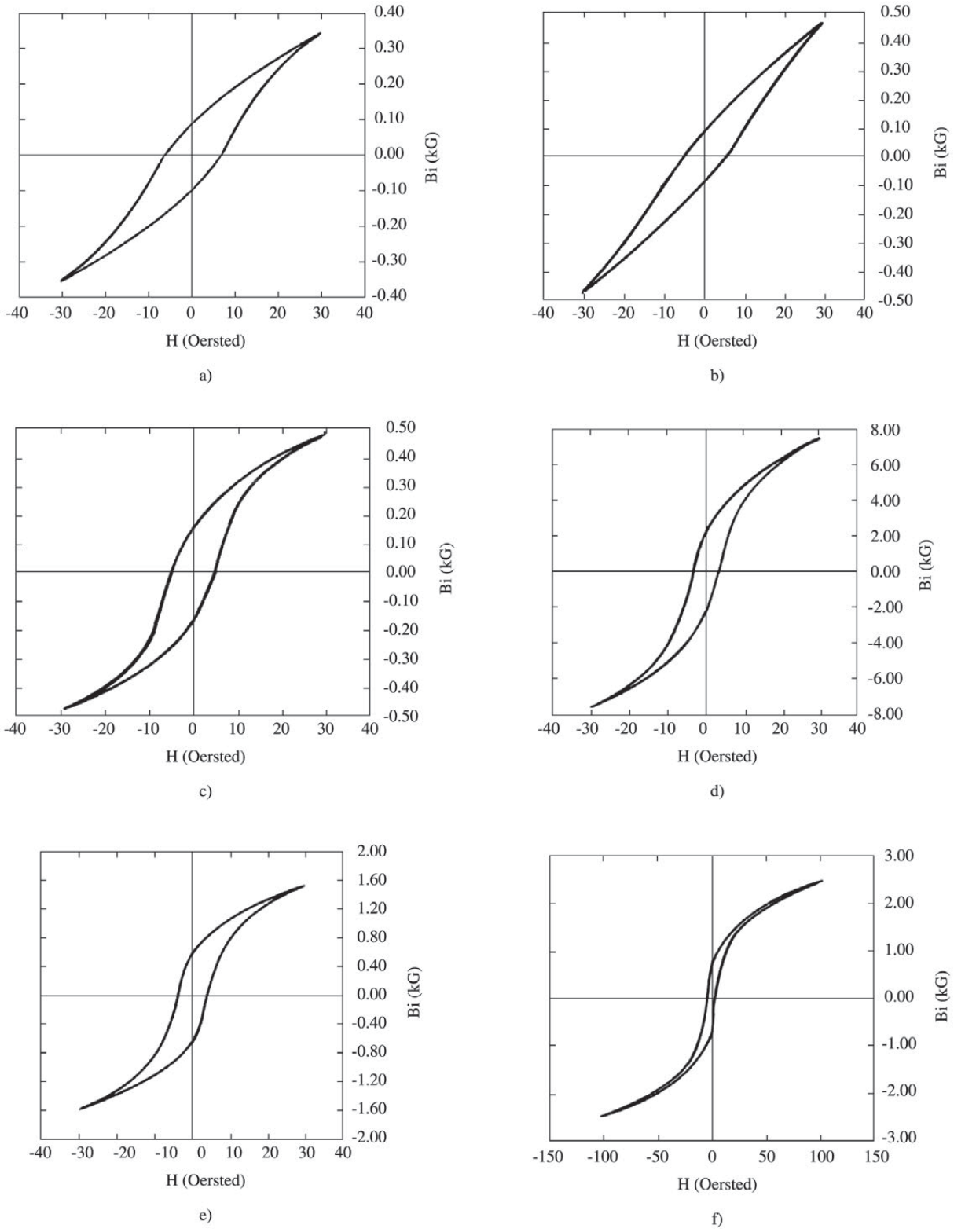

Figure 5. Magnetic hysteresis loops for $Sm_{0.6}Ho_{2.4}Fe_5O_{12}$ ceramic rings sintered at temperature "ST". a) ST = 1200 °C, Hmax = 30.50 Oe; b) ST = 1250 °C, Hmax = 30.08 Oe; c) ST = 1300 °C, Hmax = 30.44 Oe; d) ST = 1400 °C, Hmax = 30.77 Oe; e) ST = 1450 °C, Hmax = 30.27 Oe; f) ST = 1450 °C, Hmax = 103.57 Oe.

1200 °C, 10 at 1250 °C, 10 at 1300 °C, 10 at 1400 °C and 10 at 1450 °C), with each group presenting similar results. Thus, Figs. 5 and 6 depict, respectively, the magnetic hysteresis curves and scanning electron micrographs of samples sintered at different temperatures, while Tables 1 and 2 summarize the main data of the sintered ceramics for the case of x = 2.4. From the morphological standpoint, a relatively large number of pores remained in the sintered ceramic pieces, suggesting the forming and sintering processes require further improvement in order to achieve full densification.

The hysteresis loops obtained were comparable to those of the best similar garnets in the market, which show saturation magnetization in the order of 1.2 to 1.9 kG and a coercive force of about 2.5 Oe [4,16].

An examination of the hysteresis curves led to the conclusion that the coercive force decreased as the sintering temperature rose, as a result of the greater grain growth of the ceramic pieces during sintering at higher temperatures. In fact, it is clear that increasing the sintering temperature produced progressive grain growth (1.8 μm at 1200 °C to 12.0 μm at 1450 °C). However, the increase in sintering temperature also produced phase transformation, as illustrated in Fig. 4. Therefore, increasing the sintering temperature promotes both phase transformation and grain growth. Phase transformation (by nucleation and growth) should act as a grain refining process. The temperature exerts such a strong effect, however, that it can lead to substantial net grain growth.

The B_{max} and B_r values reached a maximum at 1400 °C, a situation that would have been different had a denser green compact been sintered (at a lower temperature), producing smaller grain-sizes after sintering.

Initial permeability, coercive force, switching time, effective linewidth and spinwave linewidth are well-known grain size-dependent magnetic parameters[18]. According to GLOBUS[16], who studied the correlation between the hysteresis loop and the microstructural parameters (such as grain

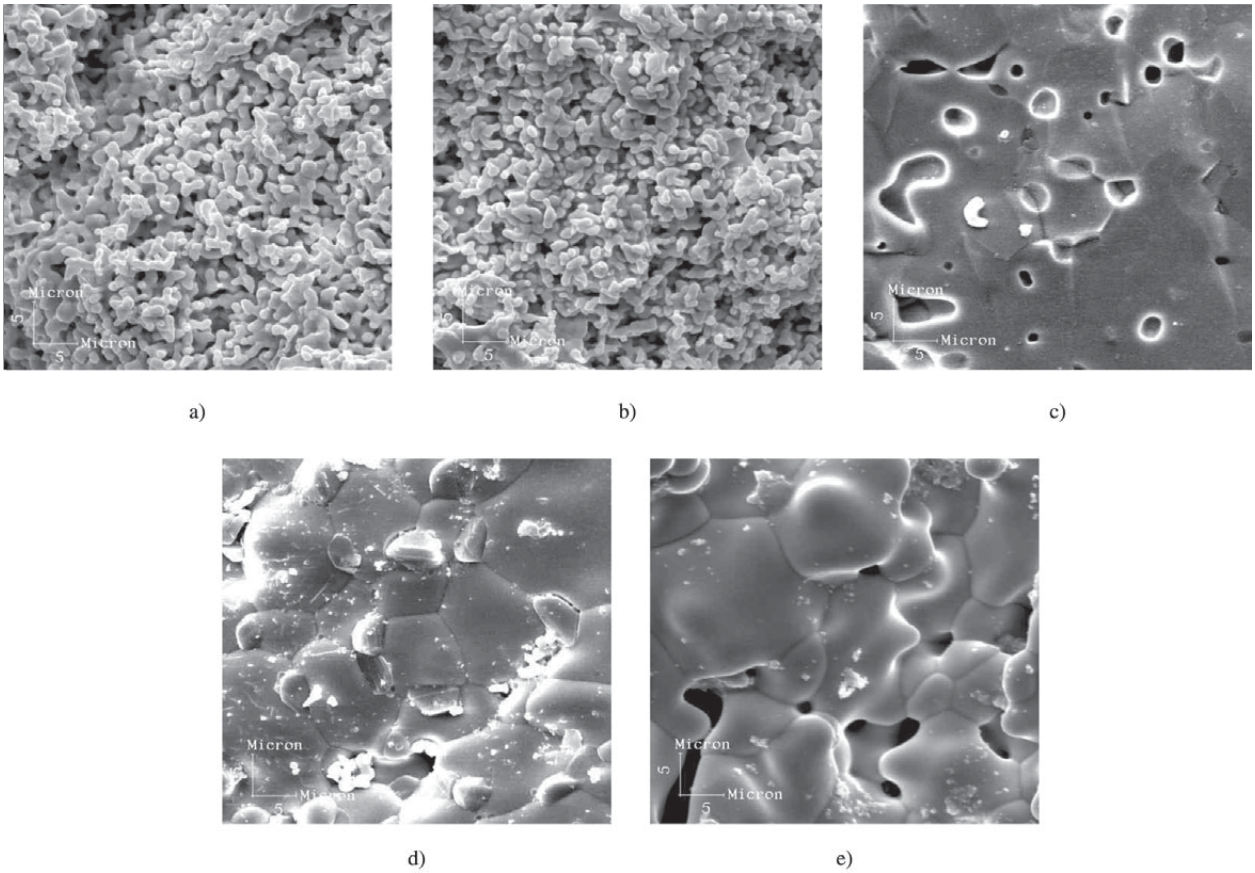

Figure 6. Scanning Electron Micrograph of the $Sm_{0.6}Ho_{2.4}Fe_5O_{12}$ rings sintered at temperature "ST". a) ST = 1200 °C; b) ST = 1250 °C; c) ST = 1300 °C; d) ST = 1400 °C; e) ST = 1450 °C.

Table 1. Analysis of results for $Sm_{0.6}Ho_{2.4}Fe_5O_{12}$ sintered pieces.

Sintering Temperature (°C)	Coercive Force, H_c (Oe)	Maximum Magnetic Field (Oe)	Hysteresis Loss, HL(J/m^3)	Maximum Induction, B_{max} (kG)	Remanent Induction, B_r (kG)	Grain Size, GS(μm)	B_s (kG) or M_s (emu/g)
1200	6.46	30.50	39.97	0.35	0.09	1.8	
1250	5.27	30.08	45.71	0.47	0.09	2.0	
1300	4.86	30.44	45.54	0.48	0.16	10.0	
1400	3.35	30.77	507.77	7.53	2.17	8.0	
1450	3.89	30.27	145.89	1.56	0.61	12.0	2.7kG (1.80 emu/g)
1450	4.11	103.54	287.23	2.49	0.68	12.0	
1450	70	1000					2.03kG (1.35 emu/g)

Table 2. Analysis of results for $Sm_{(3-x)}Ho_xFe_5O_{12}$ sintered pieces.

Sintering Temperature (°C)	X	Coercive Force, H_c (Oe)	Hysteresis Loss, HL (J/m^3)	Maximum Induction, B_{max} (kG)	Remanent Induction, B_r (kG)	Grain Size, GS(μm)
1200	0	7.99	46.62	0.31	0.11	2.0
	1.5	7.81	42.60	0.30	0.10	2.3
	2.4	6.46	39.97	0.35	0.90	1.8
	3.0					
1250	0	7.16	182.76	1.10	0.56	2.4
	1.5	4.42	37.94	0.27	0.08	2.8
	2.4	5.27	45.71	0.47	0.09	2.0
	3.0					
1300	0	6.73	201.51	1.26	0.65	2.8
	1.5	6.68	66.93	0.50	0.19	3.0
	2.4	4.86	45.54	0.48	0.16	10
	3.0	6.26	50.36	0.32	0.12	1.8
1350	0	6.57	230.62	1.51	0.76	3.1
	1.5	6.35	72.88	0.58	0.22	3.0
	2.4					
	3.0	7.41	60.33	0.43	0.15	2.2
1400	0	6.00	23.46	0.32	0.08	4.2
	1.5	6.96	32.86	0.26	0.06	3.3
	2.4	3.35	507.77	7.53	2.17	8.0
	3.0	6.56	44.07	0.37	0.12	2.5
1450	0					
	1.5	4.16	11.51	0.15	0.02	3.1
	2.4	3.89	145.89	1.56	0.61	12.0
	3.0					

size and intragranular porosity) of the yttrium iron garnet (YIG), the coercive force is inversely proportional to the average grain size. In the case reported on here, the material's coercive force decreased as the result of grain growth from 6.46 to 3.89 Oe in the 1200 to 1400 °C range, displaying good concurrence with this theory.

The saturation magnetization, Ms, was obtained by extrapolating M (1/H)- curves to 1/H = 0. The powder analyzed had been calcined at 1450 °C/5 h. The saturation magnetization value for this material is 1.35 emu/g. Figure 7 illustrates this curve.

The Curie point increases from 272.5 °C in the pure YIG

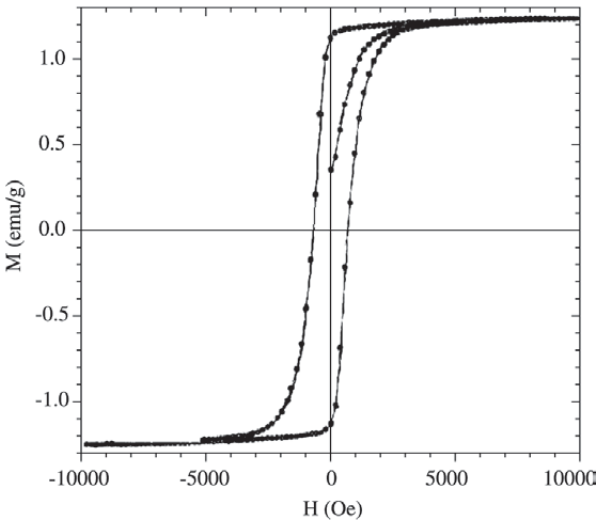

Figure 7. Hysteresis loop of the powder calcined at 1450 °C.

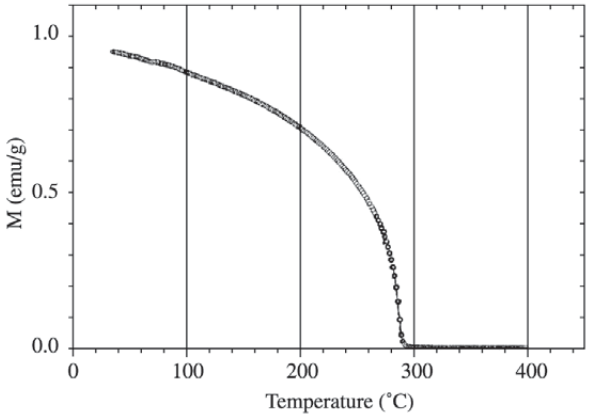

Figure 8. Magnetization-temperature curve of the powder calcined at 1450 °C when subsequently subjected to a 240 Oe magnetic field.

($Y_3Fe_5O_{12}$), reaching 289 °C in SmIG ($Sm_3Fe_5O_{12}$) [18]. Figure 8 shows the magnetization-temperature curve of $Ho_{2.4}Sm_{0.6}Fe_5O_{12}$, indicating that the Curie temperature is about 287 °C.

4. Conclusions

For the sintered toroids produced with calcined and ground powder from samarium-holmium-iron coprecipitated hydroxides, the following correlations were observed between sintering temperature and microstructure and between microstructure and magnetic properties:

(a) The grain size increased from 1.8 to 12.0 μm in the range of 1200-1450 °C.

(b) The coercive force dropped from 6.46 to 3.89 Oe in the 1200 to 1450 °C range as the result of grain growth, as expected.

(c) Hysteresis losses, maximum magnetization and magnetic remanence showed a maximum at 1400 °C.

(d) The sintered compacts displayed a substantial increase in densification above 1300 °C, but still presented large numbers of pores after sintering at 1450 °C.

(e) The calcined powder still required finer milling and sintering assisted by hot pressing in order to yield fully dense ceramics.

(f) The Curie temperature of $Sm_{0.6}Ho_{2.4}Fe_5O_{12}$ powder calcined at 1450 °C for 5 h, determined under a magnetic field of 240 Oe, is about 287 °C, a value intermediate to those of pure YIG (272.5 °C) and SmIG (289 °C), according to Aharoni *et al.*[18].

(g) The saturation magnetization of $Sm_{0.6}Ho_{2.4}Fe_5O_{12}$ powder calcined at 1450 °C for 5 h was equal to 1.35 emu/g, and was determined using a Vibrating Sample Magnetometer (measured at PAR VSM model 155).

(h) The effect of substituting samarium with holmium in SmIG on the magnetization of iron garnet differs significantly from that promoted by replacing yttrium with gadolinium in YIG, probably due to differences in the ratio of the cationic radii of the coupling non-ferrous elements. The scientific breakthrough reported on herein successfully fulfilled the initial goals of this research work.

Acknowledgements

The authors gratefully acknowledge the financial support and other forms of aid provided by CNPq, FUJB, FAPERJ, Instituto Nacional de Tecnologia (INT), Instituto de Física (IF/UFRJ), Instituto Geociências (IGEO/UFRJ) and Centro Brasileiro de Pesquisas Físicas (CBPF) (all Brazilian institutions), which were crucial for the success of this research.

References

1. Dionne, G.F.; West, R.G. "Interpretation of rare earth ion effects on spin wave linewidths of iron garnets", *Conference of Magnetism and Magnetic Materials*, v. 10, p. 169-173, 1972.
2. Rodic, D.; Mitric, M.; Tellgren, R.; Rundlof, H.; Kremenovic, A. "True magnetic structure of the ferromagnetic garnet $Y_3Fe_5O_{12}$ and magnetic moments of iron ions", *Journal of Magnetism and Magnetic Materials*, v. 191, p. 137-145, 1999.
3. Sugimoto, M. "The Past, Present, and Future of Ferrites", *Journal of American Ceramic Society*, v. 82, n. 2, p. 269-280, 1980.

4. Lax, B.; Button, K.J. *Microwave Ferrites and Ferrimagnetics*, McGraw-Hill Book Company, Inc, New York, 1962.
5. Pauthernet, T. *Spontaneous Magnetization of some Garnet Ferrites and the Aluminium Substituted Garnet Ferrites*, Journal of the Applied Physics v. 29, n. 3, p. 253-255, 1958.
6. Dionne G.F., Molecular Field and Exchange Constants of Gd^{3+} Substituted Ferrimagnetic Garnets, Journal of Applied Physics v. 42, p. 2142-2143, 1971.
7. Adair, J.H. *Filtration and Washing*, in Engineered Materials Handbook, Vol.4, Ceramics and Glasses, S.J. Schneider, *American Society for Metals International*, Columbus, OH, p.90-94, 1991.
8. Caffarena V.R.; Ogasawara, T. Synthesis of samarium-holmium-iron garnet by co-precipitation: Thermodynamic Analysis, Proceedings of 43rd Brazilian Ceramic Congress, Florianópolis-SC, Portuguese, Brazilian Ceramic Association, São Paulo-SP, Brazil, v. 1, p. 3601-3611, 1999.
9. Morita, T.; Assumpção, R.M.V. *Manual de Soluções Reagentes e Solventes. Padronização – Preparação – Purificação*, 2ª. Edição, Editora Edgard Blucher Ltda, 1972.
10. Reed, J.S. *Drying,* in Engineered Materials Handbook, Ceramics and Glasses, Samuels J. Schneider, *American Society for Metals International*, Columbus, OH, v. 4, p. 130-134, 1991.
11. Sorrel, C.A. *Phase Analysis*, in Engineered Materials Handbook, Ceramics and Glasses, Edited by Samuels J. Schneider, *American Society for Metals International*, p. 557-563, 1991.
12. Halloran, J.W. *Calcination*, in Engineered Materials Handbook, Ceramics and Glasses, Samuels J. Schneider, *American Society for Metals International*, v. 4, p. 109-114, 1991.
13. Powder Diffraction File Alphabetical Index Inorganic Compounds, Publication SMA – 27, Published by the JCPDS International Center for Diffraction Date, Park Lane, Swarthmore, Pennsylvania, 1977.
14. Forterre, G. "Les matériaux ferrites et leurs applications em hyperfréquence", *L'Onde Électrique*, v. 71, n. 1, p. 37-47, 1991.
15. Gasgnier, M.; Ostoréro, J.; Petit, A. "Rare earth iron garnets and rare earth iron binary oxides synthesized by microwave monomode", *Journal of Alloys and Compounds*, v. 277, p. 41-45, 1998.
16. Globus, A. "Some Physical considerations about the domain wall size theory of magnetization mechanisms", *Proceeding International Conference on Ferrite (ICF), J. Phys*. Supplement C1, p. C1-1 a C1-15, 1977.
17. Horvath, M.P. Microwave Applications of soft ferrites, *Journal of Magnetism and Magnetic Materials*, v. 215-216, p. 171-183, 2000.
18. Aharoni, A. *et al.* "Curie Temperature of Some Garnets by the Differential Thermal Analysis Technique", *Journal of Applied Physics*, v. 32, n. 10, p. 1851-1853, 1961.